

FIG. 6. Electron microprobe data on (a) Fe-7Mn and (b) Fe-14Mn specimens slow cooled and shock loaded at 300 kbar.

the quenched and shocked Fe-4Mn and Fe-7Mn alloys showed bcc and fcc lines, with the lattice parameters shown in Table III. The quenched and shocked Fe-14Mn alloys showed bcc and hcp phases with the lattice parameters also indicated in Table III. Six of the lines were clearly identified as hcp with a  $c/a$  ratio of 1.61. The hcp lines identified in the Fe-14Mn alloy after the 150-kbar shock had the same  $c/a$  ratio as after the 300-kbar shock. The unshocked slow-cooled Fe, Fe-0.4Mn, and Fe-4Mn specimens produced diffraction lines of bcc martensite. The unshocked slow-cooled Fe-7Mn and Fe-14Mn alloys produced hcp martensite and bcc martensite. All alloys had a 5–10% volume fraction of untransformed fcc phase. Apparently, the hcp phase in the annealed alloys is a discrete phase, very sim-

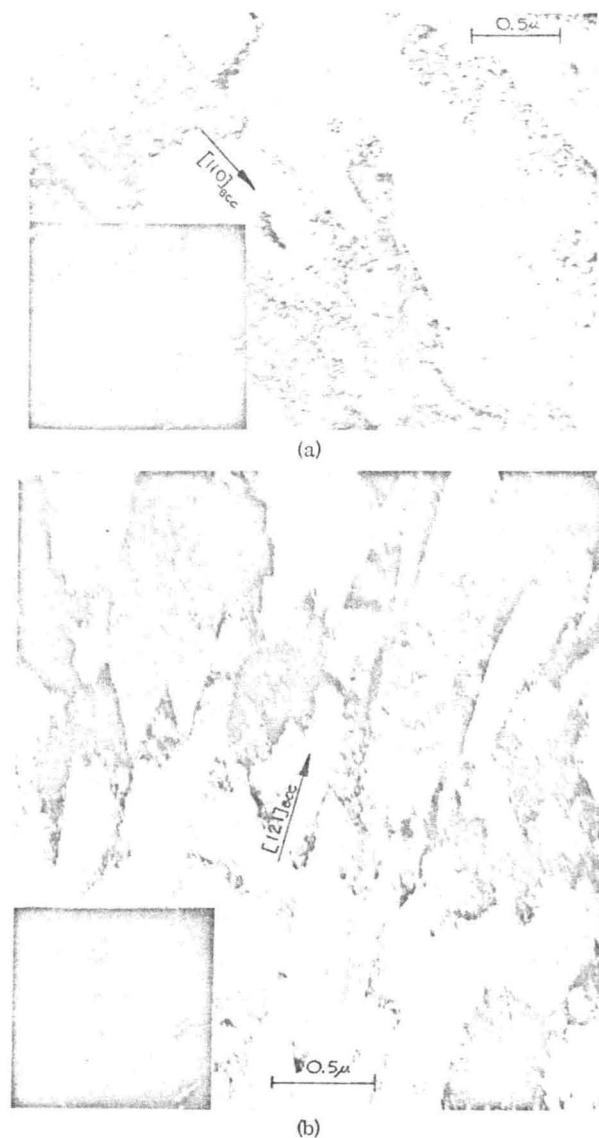


FIG. 7. (a) Electron micrograph of quenched shock-loaded Fe-7Mn at 90 kbar. The fcc plates have transformed from the initial bcc structure. The fcc plates have been identified by electron diffraction. (b) Electron micrograph of slow-cooled shock-loaded Fe-7Mn at 90 kbar.

ilar to the hcp phase in cobalt. The shock loading of the slow-cooled specimens did not produce any new lines. In addition, shock loading did not change the volume fraction of each phase present in the slow-cooled alloys.

### C. Microstructure

By light microscopy, the microstructure of all alloys was observed before and after shock loading to 300 kbar. Representative optical micrographs of the Fe-7Mn alloy are shown in Fig. 4. The typical martensitic structure prior to shock loading is shown in Fig. 4(a). The prior austenitic grain boundaries are not obvious, but with closer scrutiny of the changes in orientation of the martensitic plates, the austenitic grain boundaries become evident. After shocking, the prior austenitic grain boundaries are easily